

# Lamellar Structure and Morphology of Nylon 46 Crystals. A New Chain Folding Mechanism for Nylons

E. D. T. Atkins,\* M. Hill, S. K. Hong,† A. Keller, and S. Organ

H. H. Wills Physics Laboratory, University of Bristol, Tyndall Avenue, Bristol, BS8 1TL U.K.

Received June 10, 1991; Revised Manuscript Received October 4, 1991

**ABSTRACT:** The structure and morphology of solution grown nylon 46 crystals have been determined and compared with those of other polyamides. They have similar lath-shaped crystallization products, possessing the characteristics of chain-folded lamellar crystals with thicknesses of  $\sim 6$  nm, and often aggregate to form sheaves. Electron diffraction patterns show that the chains lie perpendicular to the lamellar surfaces and that crystal twinning occurs. Surface decoration techniques reveal for the first time in a nylon that the fold plane corresponds to the plane of the hydrogen bonds, themselves lying along the long axis of the crystal in agreement with the electron diffraction results. Sedimented mats of the crystals were examined using both wide- and low-angle X-ray diffraction in directions perpendicular to the lamellar normals. The lamellar thickness remains constant up to 125 °C and then increases with crystallization temperature  $T_c$ . Analyses of the X-ray diffraction patterns confirms without doubt that the chain stems in nylon 46 chain-folded crystals are parallel to the lamellar normal in contrast to previous results from other polyamides, e.g. nylon 66, 6.10, and 6.12 where the chain stems are inclined at substantial angles to the lamellar normal. The consequences of these findings demand an entirely new mechanism for folding in nylons, where an amide group is incorporated in the fold, rather than alkane segments as in previous chain-folded nylons. The fold exhibits similarity with the  $\beta$ -bend in proteins. The lamellar thickness is sufficient to accommodate four structural repeats of the chain. The crystallographic subcell is monoclinic, with parameters  $a = 0.96$ ,  $b = 0.826$ , and  $c$  (chain axis) = 1.47 nm and  $\gamma = 115^\circ$ , and contains four chain segments (two sheet segments), which bears similarity with the unit cell of nylon 6.

## Introduction

Nylon 46 is a member of the polyamide family with a high amide content; successive amide groups are equally spaced, but with opposite polarity, along the chain as shown in Figure 1. The chemical synthesis, melting point, and thermal behavior have been reported.<sup>1-5</sup> It is a novel engineering plastic and is currently manufactured by DSM under the trade name Stanyl. The polymer has a higher melting point and enhanced mechanical properties<sup>4</sup> compared to the more usual commercial nylons such as 66 and 6. The melting point of nylon 46 single crystals varies between 281 and 289 °C depending on the crystallization temperature (100 and 160 °C, respectively). These values are higher than the melting points of nylon 66 and 6 which are given as 265 and 215 °C, respectively. X-ray fiber diffraction patterns<sup>6</sup> of nylon 46 show that the spacing of certain reflections, in particular two strong reflections at 0.44 and 0.37 nm, are similar to nylon 66 and nylon 6.<sup>10,7</sup> with the periodicity along the chain,  $c$ , appropriately reduced to 1.47 nm.

The morphology and chain-folded structure of single crystals of other polyamides have been reported previously;<sup>8-15</sup> nylon 66 is especially important because of its commercial prominence. Nylon 66 crystals can be grown from dilute solution; they are usually lath shaped and often aggregate into sheaves. The crystals are of limited thickness (5–7 nm), so that there are few crystallographic repeat units in each crystal stem.<sup>10-15</sup> The hydrogen bonding of the CONH dipolar arrays in polyamides define sheets containing these hydrogen bonds within the internal structure of crystalline fibers.<sup>7,16</sup> The lath-like units have the characteristic attributes of chain-folded layers, yet with no conclusive evidence with regard to folding direction with respect to the morphology.<sup>9</sup> Wide- and low-angle X-ray analyses of nylon 66 single-crystal mats

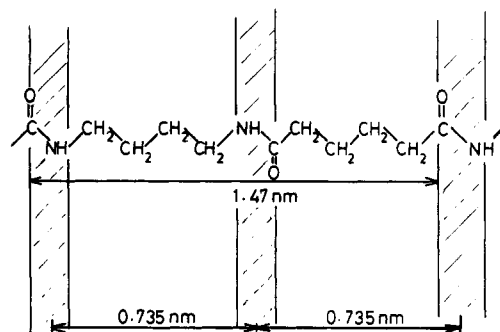


**Figure 1.** Chemical repeat of nylon 46. The chain is a planar zigzag with a length of 1.47 nm. The 46 notation relates to the four carbon atoms in the diamine portion, and the six carbon atoms in the dibasic acid portion. Note that the amide units are equally spaced at 0.735 nm along the chain which will be a feature in the proposed structure.

(together with several other nylons, but not including nylon 46) have shown that the chains within each lamella are inclined at substantial angles ( $\sim 40^\circ$ ) to the fold surfaces. Furthermore, owing to the small number of structural repeat units within the crystal stem, weaker, subsidiary X-ray diffraction maxima have been observed.<sup>10,14,15</sup> It followed from the sum total of evidence that, in the best-defined cases at least (thinnest lamellae for a given crystallization temperature), there could only be a small-chain portion within the fold, leaving no alternative to adjacent fold reentry. In order to comply with the known crystal structure within the lamellar interior this chain portion would need to be an alkane sequence, where according to the analysis of relative intensities of the subsidiary maxima, performed for nylon 66, the sequence between two contiguous CO groups is preferred.<sup>10</sup>

In this present paper we present results from our studies of solution-grown nylon 46 crystals, which show some features in common with nylon 66 and nylon 6 but differ dramatically in other respects. The most important are

\* To whom correspondence should be addressed.

† Present address: Department of Polymer Engineering, Chun-Nam National University, Tajeon, Republic of Korea.

the detailed nature of the fold itself, the direction of the straight stems in relation to the fold surface, and the crystallography of the lamellae. We will show that nylon 46 chain-folded crystals are the first in the nylon family to fold in a way which bears a resemblance to the folding behavior of proteins through  $\beta$ -bends.<sup>17-19</sup>

### Experimental Section

The commercial grade nylon 46 (Stanyl) used in this work was kindly supplied by DSM of the Netherlands, as polymer chips, free of additive.

**Single Crystal Preparation.** Solutions of nylon 46 in 1,4-butanediol (0.04% (w/v)) were prepared. Crystals were grown isothermally at various temperatures between 130 and 160 °C after self-seeding<sup>20</sup> at 195 °C. The solution was hot-filtered at the crystallization temperature after crystallization was complete. Crystals were usually dried by holding them overnight between mica plates in a vacuum oven at 70 °C. Heat treatments were carried out under nitrogen in an Abderhalden drying apparatus.

**Electron Microscopy.** TEM specimens were prepared by putting drops of crystal suspension onto carbon-coated copper grids and allowing the solvent to evaporate in a vacuum oven. Some crystals were shadowed with Pt/Pd to improve contrast for clearer observation of morphology. Other, unshadowed, crystals were used for electron diffraction. Polyethylene crystals were introduced onto the same carbon-coated grids for diffraction calibration.

Decoration techniques can provide valuable information concerning the regularity of a crystal surface or, in the case of polymers, the orientation of the folds within the surface. In the latter case surface decoration by polyethylene vapor, as developed by Wittman and Lotz,<sup>21</sup> is particularly important. In this method polyethylene is heated under vacuum and the degraded fragments produced are deposited onto the surface of single crystals. The decorated sample can then be shadowed with metal to improve contrast. The method has been most widely applied to single crystals of polyethylene and paraffin,<sup>21,22</sup> revealing fold-plane orientation and sectorization in a striking manner, but it has also been shown to be applicable to other, chemically dissimilar polymers.<sup>21</sup>

In this study, crystals of nylon 46 were deposited onto carbon-coated microscope grids, decorated with polyethylene, and shadowed with Pt/Pd for examination by transmission electron microscopy. A light coating of polyethylene was found to be most appropriate for the rather small nylon crystals available. A Phillips 301 transmission electron microscope, operating at 80 kV, was used for observation.

**X-ray Diffraction.** Single-crystal mats were examined using both wide- and low-angle X-ray diffraction techniques. Pinhole collimation and photographic film was used and the camera evacuated to reduce air scatter. Low-angle X-ray patterns were recorded using a Rigaku Denki camera. Ni-filtered Cu K $\alpha$  sources were employed throughout. Some specimens were dusted with calcite for calibration purposes.

### Results

**Morphology and Electron Diffraction.** Figure 2 is a micrograph of a shadowed crystal entity of nylon 46 as deposited from solution. It is a sheaf with single-crystal-like, lath-shaped extremities. In some preparations the nylon 46 crystals grow individually rather than in clumps; some of these are seen in the micrographs of decorated samples, as shown in Figure 3 for example. These crystals look similar to those of nylon 66 where the laths were identified as single crystals by electron diffraction, as far back as 1964 (Holland<sup>23</sup>) and in subsequent works. In nylon 66 the hydrogen-bonded sheets were found to run along the long axes of the crystals.<sup>23,8</sup>

Electron diffraction patterns from the isolated crystals or the tips of the nylon 46 sheaves again confirm the single-crystal character of the laths, in the first instance by the spot nature of the reflections (Figure 4a). The pattern is

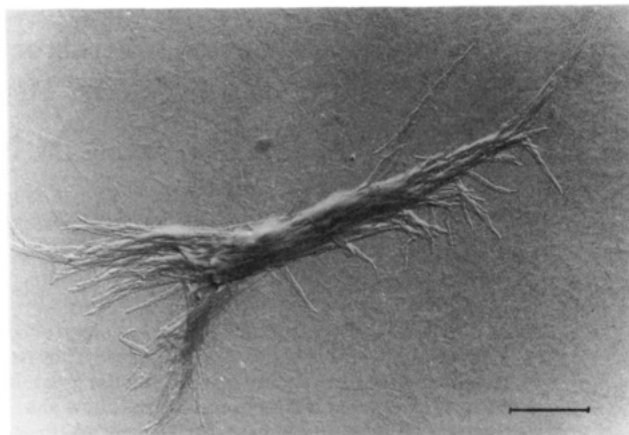


**Figure 2.** Transmission electron micrograph of a sheaf of nylon 46 crystals prepared from 1,4-butanediol.

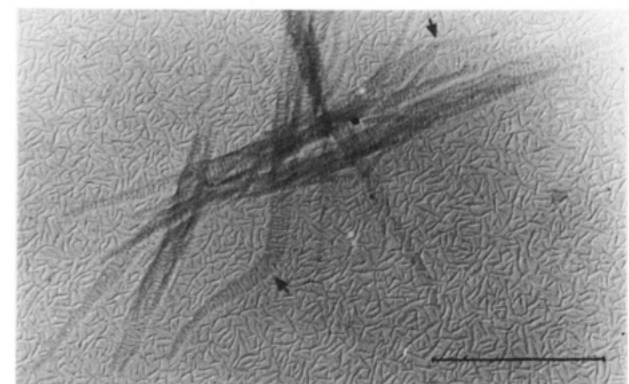


**Figure 3.** Electron micrograph of nylon 46 crystals grown at 130 °C, decorated with polyethylene using the Wittmann and Lotz<sup>21</sup> technique and shadowed with Pt/Pd. A number of crystals (arrowed) were noticed to bend at a discrete angle of 132°.

slightly complicated by twinning of the lattice. Six independent reflections can be seen in the best negatives; they are oriented as shown in the drawings: Figure 4c to be read in conjunction with Table I where the spacings measured from electron diffraction are listed and Figure 4d which also shows the orientation of the crystal with respect to the diffraction pattern. The two strongest reflections are spaced at 0.435 and 0.375 nm and lie at an angle of 65° to each other. Note in Figure 4c and Table I the 210 reflection (too weak to appear in photographic reproduction) at 0.235 nm which emanates from the interchain repeat in the hydrogen bonded sheets and provides further support for our argument that the chains are perpendicular to the lamellar surfaces. The electron diffraction pattern of nylon 66 (Figure 4b) is added here for comparison (see discussion below). In nylon 46 twinning of reflections occurs about a line perpendicular to the direction of the 0.375-nm reflection. We were interested to find that all the nylon 46 crystals we observed were twinned. Kovacs et al.<sup>24</sup> also found extensive twinning in polyethylene oxide single crystals which they discussed in terms of the excess surface energy required for forming the twin boundaries; they observed twins to be particularly numerous when the crystal preparation had been seeded. Our nylon 46 crystals were all grown by the self-seeding technique.

The results of polyethylene decoration of nylon 46 crystals are from crystals grown at 130 °C from 1,4-butanediol after self-seeding at 195 °C, but similar results were obtained from other preparations. Figure 3 shows a typical selection of decorated crystals. The decoration pattern reveals a regular feature in the form of striations

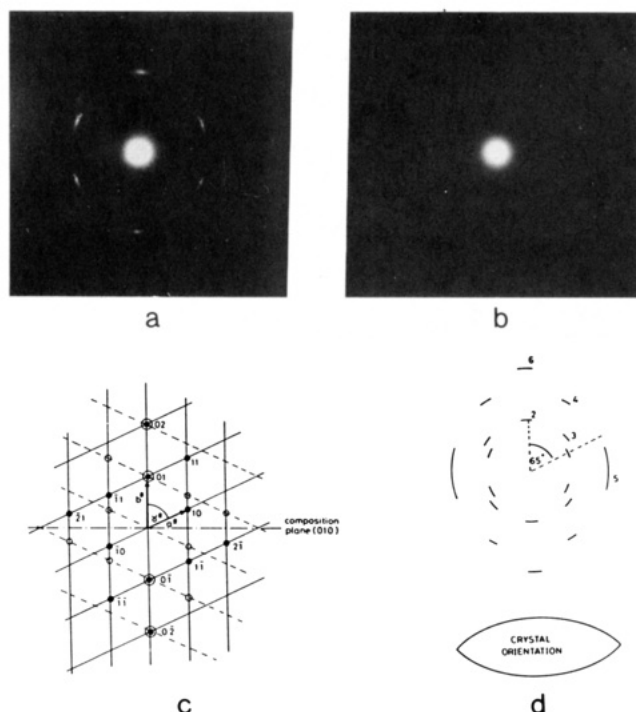


**Figure 4.** Selected area electron diffraction pattern from crystals of nylon: (a) Nylon 46 taken at the extremity of a sheaf. The closely spaced multiple spots indicate several diffracting crystals in slightly different orientations. (b) Nylon 66 taken at the extremity of a sheaf. The pair of (100) diametrically opposite reflections are at spacing 0.44 nm. The diffraction ring is from the metal Pt/Pd shadowing. (c) Drawing of the reciprocal net for nylon 46 chain-folded crystals. The filled circles index on a reciprocal lattice ( $hk0$ ) with  $a^* = 2.30$  and  $b^* = 2.67$  nm<sup>-1</sup> and  $\gamma^* = 65^\circ$ , or, in real space,  $a = 0.48$  and  $b = 0.413$  nm and  $\gamma = 115^\circ$ . Analysis of the X-ray diffraction data (later) will show that in the true unit cell  $a$  and  $b$  will need to be doubled. The reflections are twinned about the (010) composition plane, and these reflections are indicated with open circles. Where twinned reflections overlay, both symbols are shown. (d) Drawing of single crystal (bottom) in relationship to the diffraction pattern (top). The hydrogen-bonded sheets run parallel to the (010) plane and therefore parallel to the long axis of the crystal.

**Table I**  
Data from Electron Diffraction of Nylon 46<sup>a</sup>

reflection number <sup>b</sup>	measured spacing, nm	estimated relative intensity <sup>c</sup>	index <sup>d</sup>
1	0.435	VS	10
2	0.375	S	01
3	0.372	M	1 $\bar{1}$ (twin)
4	0.240	W	11
5	0.235	W	2 $\bar{1}$ and twin combination
6	0.188	W	02

<sup>a</sup> Spacings were determined by comparison with polyethylene single crystals deposited on the same carbon-coated grid. All the recorded reflections are shown in Figure 4d, but only the reflections listed as 1–3 below are visible in the photographic reproduction (Figure 4a).

<sup>b</sup> See Figure 4d. <sup>c</sup> VS = very strong. S = Strong. M = Medium. W = Weak. <sup>d</sup> The  $hk0$  net indexes on a lattice with  $a = 0.48$  and  $b = 0.413$  nm and  $\gamma = 115^\circ$ .

perpendicular to the long faces of the crystal. By analogy with the results from polyethylene<sup>21,22</sup> we interpret this as indicating that the nylon chains are folded parallel to the long axes of the crystals. From the orientation of the electron diffraction patterns with respect to the crystals, we believe that this indicates that folding takes place along the planes running parallel to the long axes of the crystals which have been shown, by electron diffraction, to be the hydrogen-bonded sheets.

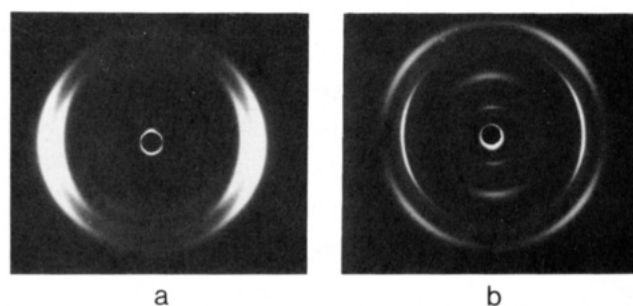


**Figure 5.** Wide-angle X-ray diffraction patterns of sedimented mats of chain-folded nylon crystals. The normal to the mat (and also to the lamella) is vertical. The lamellae are in random orientation about the mat normal and so the patterns exhibit cylindrical symmetry: (a) Nylon 46 crystals. Note the two strong interchain spacings at 0.44 and 0.37 nm (see Table I) are on the equator. In this particular pattern the reflections are broad indicating that the crystals are small. (b) Nylon 66 crystals. In this case the two strong lateral (interchain) spacings are split and lie off the equator. In the pattern the relative splitting of the inner of these two reflections is not particularly noticeable owing to overlap of the arc tails. Note also that the meridional signals are quite different from the pattern of nylon 46. The two most intense meridional arcs are 001 and 002. The two equispaced weak reflexions between are the subsidiary maxima referred to in the text.

To summarize the morphological, diffraction, and polyethylene decoration evidence from electron microscopy: the basic units are lath-shaped, chain-folded layers; the nylon 46 chains lie normal to the basal crystal faces; the hydrogen-bond containing sheets run parallel to the long axis of the crystal; and the chains fold along these hydrogen-bonded sheets.

**Wide-Angle X-ray Diffraction.** A wide-angle X-ray diffraction pattern from a sedimented mat of nylon 46 crystals is shown in Figure 5a and the corresponding pattern from nylon 66 is shown in Figure 5b. There are several common features. First, there are arcs on the equator, the strongest of these spaced at 0.435 and 0.37 nm, spacings characteristic of the lateral separation of the chains in nylons. Second, in both cases, there are arcs on or about the meridian. These are reflections associated with the periodicity along the chain.

Several significant differences between parts a and b of Figure 5 are also observed.

i. The reflections at 0.37 nm (due to the hydrogen-bond sheet separation) are split in the nylon 66 pattern although not split in the nylon 46 pattern. In the present context this means that in nylon 46, but not in nylon 66, the chains are perpendicular to the lamellar surfaces (as was shown by the electron diffraction patterns).

ii. The character of the meridional reflections is different. Several inner reflections are missing in nylon 46, including the subsidiary maxima which are distinctive features of the chain-folded nylon 66 diffraction pattern.<sup>10</sup>

The spacings and positions of the reflections that we have observed from sedimented single-crystal mats of nylon 46 are listed in Table II.

**Low-Angle X-ray Diffraction.** A low-angle X-ray photograph, taken after crystallization at 110 °C, is shown in Figure 6; patterns of similar appearance, but sometimes different spacing, are found on crystallization at other temperatures. These patterns were taken with the beam parallel to the mat plane; they show arced reflections on the meridian (i.e., along the mat normal), indicating stacks of lamellae, as usually found in crystal mats. The long spacing of a mat originally crystallized at 110 °C was 7.0 nm, and reduced to 6.2 nm on annealing at 230 °C. By analogy with previous work on nylons 66, 6.10, and



Table II  
Wide-Angle X-ray Diffraction Data of Nylon 46<sup>a</sup>

index	measured spacing, nm	calculated spacing, nm
Equator		
200	0.437	0.435
020	0.371	0.374
220	0.236	0.238
420		0.236
Second Layer Line		
002	0.732	0.735
012	0.530	0.524

<sup>a</sup> The prominent diffraction signals are listed together with the indexing based on a monoclinic unit cell with parameters  $a = 0.96$ ,  $b = 0.826$ , and  $c$  (chain axis) = 1.47 nm and  $\gamma = 115^\circ$ .

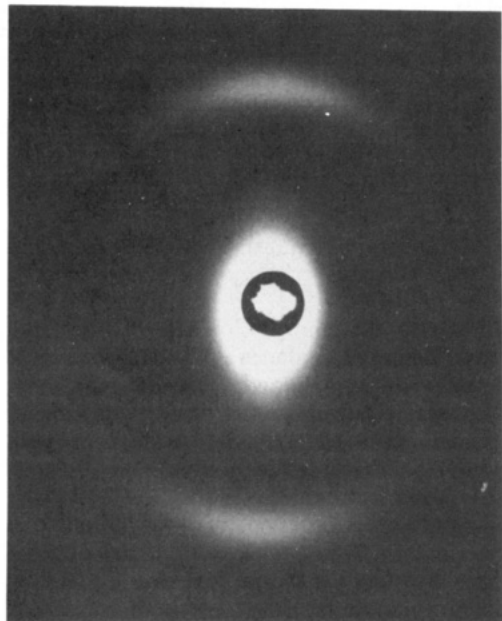


Figure 6. Low-angle X-ray diffraction pattern of a sedimented mat of nylon 46 chain-folded crystals which had been crystallized from 1,4-butanediol at 110 °C. On the actual negative a weak second order is visible.

10,10,<sup>9-11</sup> we interpret this reduction as being due to improved lamellar packing, and, accordingly, take the lowest (annealed) spacing as a measure closest to the actual thickness of an individual lamella.

When looking for a connection between lamellar thickness and a molecular parameter, the most conspicuous feature presenting itself is that the long period corresponds to only a little more than 4 chemical repeat units ( $4 \times 1.47 = 5.88$  nm) along the chain.

In Figure 7 we show the low angle spacing ( $L$ ) as a function of crystallization temperature ( $T_{cr}$ ). We see that  $L$  is constant at low  $T_{cr}$  (corresponding to the four chemical repeats referred to above), but  $L$  becomes an increasing function of  $T_{cr}$  for crystallization at 130 °C and upward. This pattern of a horizontal plateau in  $L$ , followed by a gradual rise, parallels the previously observed behavior of nylons 66 and 6.10.<sup>9,15</sup>

## Discussion

In this discussion we first analyze the data obtained from TEM, in particular considering the implications of the electron diffraction results in terms of the orientation of the chains with respect to the lamellar surfaces. The X-ray diffraction evidence will be presented in the context of the previously proposed models for nylon 66 and 6 in order to highlight the important differences between the

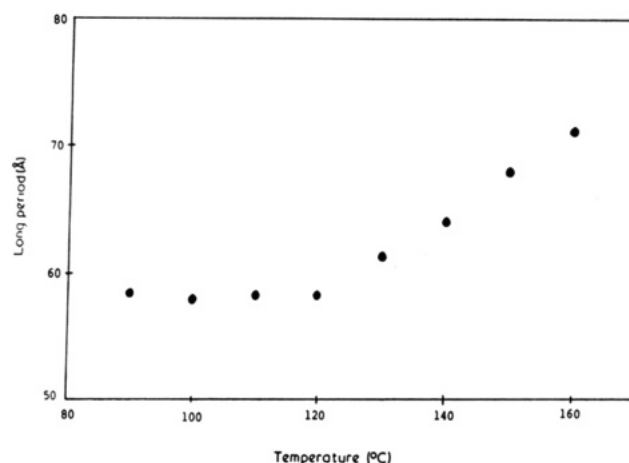


Figure 7. The dependence of the long period of nylon 46 crystals ( $L$ ), measured by low-angle X-ray diffraction, on the crystallization temperature  $T_{cr}$ .

chain folding mechanism in nylon 46 compared with the other nylons.

**Analysis of TEM Data.** We know from our electron microscopy, including imaging, decoration, and electron diffraction, that the basic crystal lamellae are lath-shaped, chain-folded layers. The nylon 46 chains lie normal to the basal crystal faces. The hydrogen-bond containing sheets run parallel to the long direction of the crystal and the chains fold along these hydrogen-bonded sheets.

The unit-cell parameters can be determined from the  $hk0$  reciprocal lattice revealed by electron diffraction. A drawing of this lattice is shown in Figure 4c and the spacings and indexing listed in Table I. The electron diffraction signals index on a lattice with parameters  $a = 0.48$  and  $b = 0.413$  nm and  $\gamma = 115^\circ$ . (We are using the appropriate crystallographic nomenclature of an obtuse angle for a real space lattice.) There is a slight complication because the lattice is twinned, with a composition plane (010). Since the  $hk0$  reciprocal net is insensitive to shears parallel to  $c$  the reciprocal lattice degenerates to a one-chain unit cell. In the X-ray analysis later we will show that the  $a$  and  $b$  values will need to be doubled and the full three-dimensional unit-cell established. The hydrogen-bonded sheets lie in the  $ac$  plane.

**X-ray Diffraction from Sedimented Mats.** The interpretation of the X-ray diffraction patterns from sedimented mats of nylon 46, consisting of stacks of chain-folded lamella, is aided by an understanding of the salient features of the crystal structures of nylon 66 and 6.10 found in fibers.<sup>7</sup> Indeed, when the details of adjacent reentry folding are considered later, comparison with the X-ray results from both nylon 66 fibers<sup>7</sup> and sedimented mats<sup>10</sup> will become important and a discussion of the structures for nylon 6<sup>16</sup> and the  $\beta$ -sheet protein structures will be necessary.<sup>17,18</sup> In order to present our analysis of nylon 46 it is essential to outline the salient features of nylon 66 and nylon 6.

**Nylon 66 Crystal Structure in Fibers.** The structure and crystallographic details are shown in Figure 8. The basic structural ingredients are extended, zigzag-like chains, which zip together through linear hydrogen bonds between the amide groups to form sheets. The subtle and specific hydrogen bonding pattern results in a progressive relative stagger between the chains and parallel to the chain direction, i.e. the  $c$  direction ( $\sim c/14$  in the case of nylon 66 and  $\sim c/18$  for nylon 6.10), within the hydrogen-bonded sheet. Successive sheets close pack, and the nature of the van der Waals interactions and distribution of amide

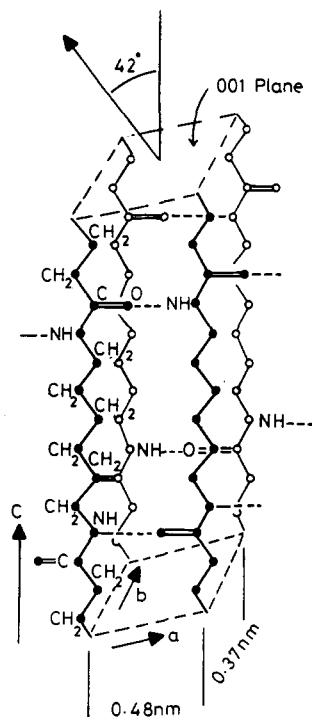


**Figure 8.** Unit cell of nylon 66 after Bunn and Garner.<sup>7</sup> The cell is triclinic with parameters  $a = 0.49$ ,  $b = 0.54$ , and  $c$  (fiber axis) =  $1.72$  nm and  $\alpha = 48.5^\circ$ ,  $\beta = 77^\circ$ , and  $\gamma = 63.5^\circ$ . Linear hydrogen bonds between amide units connect the planar zigzag chains together at a separation of  $0.48$  nm to form a hydrogen-bonded sheet in the  $ac$  plane. The hydrogen bonding scheme imparts a progressive shear of  $\sim c/14$  in the  $c$  direction. The sheets close pack at a distance of  $0.37$  nm and are progressively sheared in both the  $c$  direction and in a direction perpendicular to  $c$  in the  $ac$  plane creating the primitive triclinic unit cell. The high electron density interchain planes are the  $(100)$  planes at a spacing of  $0.44$  nm and the  $(010)$  intersheet planes at spacing  $0.37$  nm. The other significant planes are the  $(00l)$  planes, the  $002$  reflection being the strongest, the normal to which lies at an angle of  $\sim 42^\circ$  to the  $c$  axis.

groups induce a progressive intersheet shear (like a sheared pack of playing cards), with components in both the  $c$  direction and in a direction perpendicular to  $c$  and in the  $ac$  plane. The result is a triclinic unit cell, the details and crystallographic parameters are given in the legend to Figure 8. From an X-ray diffraction point of view, the strongly scattering planes are those parallel to the chain axis ( $c$  direction), in particular the  $100$  reflection at spacing  $0.439$  nm, the  $010$  reflection at  $0.373$  nm, and the  $110$  reflection at  $0.366$  nm. The latter two reflections are usually unresolved and so there is a rather straightforward and distinctive X-ray fingerprint for nylons in this category, i.e. two strong equatorial diffraction signals at spacing  $0.44$  and  $0.37$  nm. The  $0.37$ -nm diffraction signal represents the intersheet distance and the  $0.44$ -nm signal is a projected value (caused by the progressive intersheet shearing) of the  $0.48$ -nm interchain distance within the hydrogen-bonded sheet (see Figure 9). This latter dimension is a key feature of sheets utilizing simultaneous donor and acceptor *linear* hydrogen bonds via amide groups and is also a classical element in the  $\beta$ -sheet proteins.<sup>18</sup> One other set of diffraction signals are of significance: the  $00l$  set of reflections, the  $002$  being the strongest for nylon 66 at a spacing of  $0.64$  nm, which emanate from planes passing through amide groups. The  $(002)$  plane is inclined at a substantial angle ( $\sim 42^\circ$  for nylon 66) to the  $c$  direction as illustrated in Figure 8. This is the  $\alpha$  form<sup>7</sup> of nylon 66.

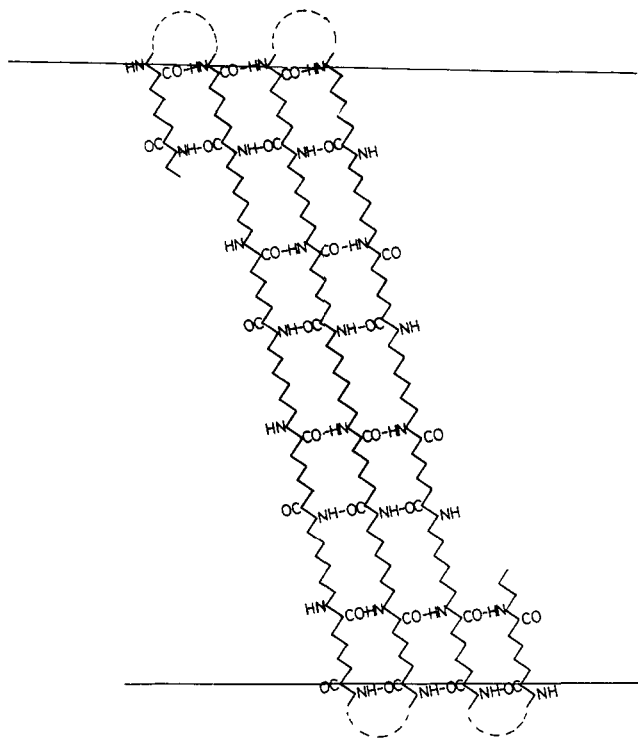


**Figure 9.** Details of a chain-folded sheet of nylon 66.<sup>10</sup> The chains fold via the alkane segments in the chain and since adjacent chains progressively shear in the  $c$  direction by  $\sim c/14$  the normal to the fold plane is automatically inclined at an angle to the chain direction. Consequently, when lamellar crystals are sedimented to form mats the chain segments ( $c$  direction) are inclined to the mat normal. In practice the additional intersheet shear increases the inclination angle to  $42^\circ$ .

**Nylon 66 Chain-Folded Lamella.** The consequences of incorporating equivalent and adjacent reentry folds into the nylon 66 crystal lattice are illustrated in Figure 9. This is shown in two dimensions as projected onto the  $(010)$  plane with a projected inclination of  $13^\circ$ . Thus when such lamellae stack in sedimented mats, the chains, or to be precise the straight stem chain segments, are tilted with respect to the lamellar normal (hence the mat normal) by the angle of  $42^\circ$  (see Figure 8) and the fold surfaces are parallel to the  $(001)$  planes. Thus, compared with a fiber (as above), a bulk rotation occurs of the crystallographic lattice and  $00l$  reflections appear along the sedimented mat normal (meridian) as seen in Figure 5b.<sup>10</sup> The  $100$  and  $010$ ,  $110$  unresolved pair no longer appear on the equator but split and straddle the equator. This is far more prominent for the  $010$ ,  $110$  pair at  $0.37$  nm where the split is  $\sim \pm 40$ – $50^\circ$  compared with the  $100$  split  $\sim \pm 13^\circ$ . Two other diffraction features overlay these signals:

- (i) The stacking of the lamellae produces a low-angle diffraction pattern on the meridian—a superlattice, the quality and position of which is a function of annealing.
- (ii) The limited number of crystallographic repeats along the chain segments, typically four for nylon 66,<sup>10</sup> produce subsidiary maxima, again on the meridian.

From these results it is obvious that the chains are *not* perpendicular to the chain-folded lamella and that electron diffraction of a lamella lying on a grid, with the beam perpendicular to the lamella, will *not* reveal the characteristic  $0.44$ - and  $0.37$ -nm diffraction signals.

**Nylon 6 Crystal Structure in Fibers.** The model proposed for nylon 6 fibers<sup>16</sup> differs from nylon 66 and three features have relevance to our nylon 46 results, to be discussed in detail shortly.

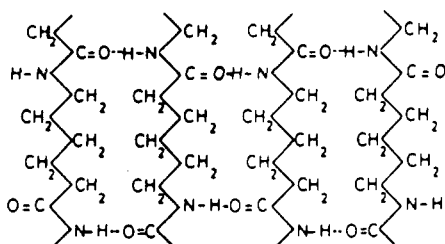


Figure 10. Structure proposed for the hydrogen-bonded sheet of nylon 6.<sup>16</sup>

(i) The linear hydrogen-bond pattern within a hydrogen-bonded sheet staggers alternatively up and down between adjacent chains and is not progressive as in nylon 66 (see Figure 10).

(ii) The chain in nylon 6 has a polarity, so adjacent chains are antiparallel, analogous to the antiparallel pleated sheets in proteins.<sup>17,18</sup>

(iii) Successive sheets do not progressively shear but shear first one way and then with the opposite shear vector resulting in a two-sheet structural repeat.

The consequences of these factors give rise to a monoclinic unit cell with parameters  $a = 0.956$ ,  $b = 0.801$ , and  $c$  (fiber axis) =  $1.724$  nm and  $\gamma = 112.5^\circ$ . Note that the  $a$  and  $b$  dimensions are effectively doubled compared with nylon 66 and the obtuse angle is chosen for  $\gamma$  in accordance with crystallographic convention for monoclinic systems. Again the  $0.44$ -nm (now indexed as the 200 reflection) and the  $0.37$ -nm (020 and 220 unresolved pair) reflections are the prominent interchain diffraction signals.

**Nylon 46 Sedimented Mats.** The X-ray diffraction pattern exhibits the two characteristic  $0.44$ - and  $0.37$ -nm diffraction signals on the equator (see Figure 5a). This means that the chain direction is perpendicular to the lamellae surface and is in agreement with the electron diffraction results obtained from individual lamellae (see previous TEM section). In fact the X-ray pattern is quite similar in general features to the published X-ray diffraction patterns of both nylon 66 fibers<sup>7</sup> and nylon 6 fibers.<sup>16</sup> If an adjacent reentry chain-folded model for nylon 46 is constructed, analogous to the model for nylon 66, with due allowance for the reduction in the  $c$  dimension, then an obvious dilemma arises: the fold surfaces are inclined by a substantial angle to the chain direction along the lines visualized in Figure 8. This would be in conflict both with the electron diffraction of individual lamellae (Figure 4), indicating chains normal to the lamellar surfaces, and to the low-angle X-ray diffraction (Figure 6) which confirms that the lamellar stacking direction is parallel to the chain direction. The apparent problem is resolved by considering the possible adjacent reentry folding mechanisms for nylon 46.

**A New Model for Adjacent Reentry Folding in Nylons.** Any model based on nylon 66 hydrogen-bonded sheet structure will give rise to fold surfaces inclined to the chain direction if the folds are all stereochemically similar. This is a direct consequence of adjacent reentry folding and the exact matching of hydrogen-bonding groups systematically decorating the chains. Now there is another way of zipping up extended nylon 46 chains into hydrogen-bonded sheets, a fragment of which is shown in Figure 11. Again all hydrogen bonds within the sheets are satisfied and are linear. It is a scheme closely analogous to nylon 6 fibers and the  $\beta$ -sheet proteins<sup>17,18</sup> and has in the past been considered as an alternative model in nylon 66<sup>7</sup> fibers. The sheets have rather similar characteristics: the distance between the chains is the same as for nylon 66 and nylon 6, i.e.  $0.48$  nm, and the intersheet packing

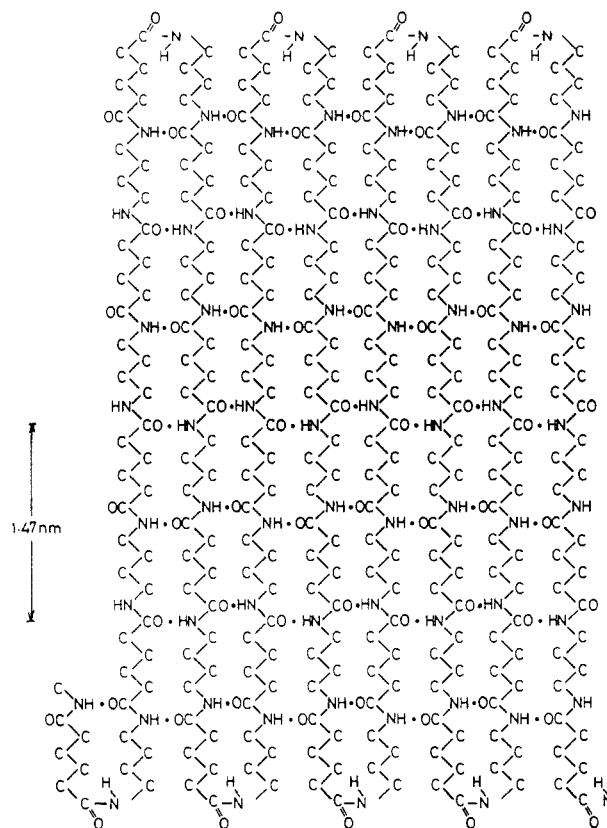


Figure 11. Structure of proposed chain-folded sheet of nylon 46. Note the amide groups in the fold. Examination of a region of the straight stems shows how the linear hydrogen bonds between amide groups lie in bands parallel to the fold surface with successive amide groups with opposite polarity. This itself is not new, it was realized first in the  $\beta$ -proteins<sup>25,26</sup> and also by Bunn and Garner<sup>7</sup> and is the basis of the proposed nylon 6 structure<sup>16</sup> and also realized independently for nylon 46 specifically.<sup>27,28</sup> What is new is that this type of two-dimensional crystallography demands a different type of folding mechanism with an amide group in the fold. Detailed computer calculations involving space filling modeling show that the outermost thickness of a lamella is  $6.0$  nm.<sup>29</sup>

distance would be expected to be close to  $0.37$  nm. There are two elements in this structure, which can be seen by inspection of Figure 11. First, amide groups do not progressively stagger between chains. Secondly, at any particular interchain amide bonding site, close neighbor amide groups have opposite polarity. This is quite different from the arrangement described for nylon 66 but rather similar to the model proposed for nylon 6.<sup>16</sup> In previous investigations and discussions on chain folding in nylons, e.g., refs 10 and 11, the explanation of the results has been compatible with the crystallography of nylon 66 since the fold surfaces created are inclined at an angle ( $\neq 90^\circ$ ) to the chain direction. Implicit in this line of reasoning is that the chains fold in the alkane segments of the chains so that consideration of the straight-stem crystallography and hydrogen-bonding mechanism is not influenced by the adjacent reentry folds. For nylon 46 chain-folded crystals we propose an entirely new folding mechanism which we judge is compatible with the experimental data. In the two-dimensional arrangement shown in Figure 11 an amide group is placed in the *actual* fold. (This is different to the "amine fold" discussed for sedimented mats of nylon 66.<sup>10</sup> In that case the fold was made through  $\text{CH}_2$  units with the  $\text{NH}$  groups residing at the entrance and exit of the fold. It was used to distinguish the fold from the "acid fold" where the  $\text{CO}$  groups occurred

at the entrance and exit positions of the fold.) We know this is stereochemically feasible since it is similar to the  $\beta$ -bend<sup>17</sup> in proteins. Proteins themselves are a kind of nylon; polyglycine is nylon 2 and a protein is a chemically decorated nylon 2. Indeed the extra CH<sub>2</sub> units either side of the amide unit in nylon 46 makes the topological task of folding even easier than for proteins. The model incorporates hairpin folds. We can rule out loose folding models since the lowest values of the stacking periodicity of lamella is 6.2 nm, only marginally greater than the size of a lamella with four times the *c* repeat of 5.88 nm. The folds have to be hairpin-like.

At a stroke we have created a chain-folded lamella where the fold surfaces are perpendicular to the chain direction, in accordance with the basic crystallographic and morphological demands of the experimental data. The effect of eliminating a complete amide group from the straight stem chain segments (by incorporating it in the fold) reverses the order of the CO and NH groups in matching amide groups in adjacent chains which facilitates this particular nylon sheet structure. There is one other vital stereochemical constraint that has to be satisfied: that the particular linear frequency of donor and acceptor groups in the amide units are exactly matched between adjacent chains. For this, the number of CH<sub>2</sub> groups between the NH and the CO groups (i.e., within the diamine and diacid) has to be equal which is indeed the case for nylon 46 as seen in Figure 11. Now it must be remembered that Figure 11 only shows a single hydrogen-bonded sheet. The adjacent sheet will inevitably be sheared relative to its neighbors along the general lines of the previous discussion regarding nylon 6 and nylon 66. However, we know *a priori* that the shear cannot have a progressive component in the chain direction since that would tilt the fold plane normal relative to the chain direction and such a feature is contrary to the experimental results and therefore we would expect sheets to successively shear up and down, an arrangement similar, but not identical, to that proposed for the  $\alpha$ -form of nylon 6 and  $\beta$ -form of nylon 66.<sup>16,7</sup> (Diffraction effects attributed to the  $\beta$ -form, both in nylon 66 and nylon 6, are accountable, and in our opinion more satisfactorily so, by considering the diffraction from hydrogen-bonded sheets stacked parallel but uncorrelated along the chain direction.<sup>30</sup>)

#### Other Structural Considerations and Implications.

**1. Subsidiary Maxima.** The small number ( $\sim 4$ ) of crystallographic repeats within the nylon 66 chain-folded lamella produced subsidiary maxima which were useful in the structural analysis.<sup>10</sup> The ratio of the *c* repeat to the lamellar thickness in the present case of nylon 46 indicates four repeats, yet no subsidiary maxima are observed. The explanation for this can be inferred from examination of Figure 11. If horizontal lines are mentally drawn through the amide groups there are at least seven equally spaced scattering planes (nine if one gives partial electron density weighting to the folds which contain an amide group). Theoretically this would give rise to  $\geq 5$  exceedingly weak subsidiary maxima ( $< 2\%$  of principle maxima intensity, i.e. 002) which we would not expect to observe above background in the data we have collected. In addition, the shear component in the *c* direction of the adjacent sheet, not shown in Figure 11, will reduce the overall intensity of even the 002 reflection, since it is anticipated to be nonprogressive, i.e., staggered. The relatively large number of scattering planes in nylon 46 is a consequence of the equal number (4) of CH<sub>2</sub> units separating the amide groups in a chain. In other words it is a special case within this category of nylons.

**2. The Unit Cell.** The task of determining the unit-cell parameters for nylon 46 is straightforward since we have direct access to the *hk0* reciprocal lattice from the electron diffraction data. Analysis of the reflections obtained from the wide-angle X-ray diffraction pattern (Figure 5a) show that the true unit cell contains four-chain segments (or two-sheet segments) and the *a* and *b* values need to be doubled. Using the X-ray diffraction pattern to measure *c* and the data from electron diffraction (see previous section on TEM) the full three-dimensional monoclinic unit cell parameters are *a* = 0.96, *b* = 0.826, and *c* (fiber axis) = 1.47 nm and  $\gamma = 115^\circ$ . These values (except for *c*) are similar to nylon 6 fibers.<sup>16</sup> A list of the main reflections is given in Table II. The calculated density is 1.24 g/cm<sup>3</sup>. This should provide an improved reference point for the rather problematic issue of defining the degree of crystallinity. We note that an experimental density as measured on fibers has been reported<sup>6,28</sup> as high as 1.231 g/cm<sup>3</sup>.

**3. Origin of Strong Diffraction Signal on Second Layer Line.** In the nylon 66 fiber structure the 002 reflection is a dominant feature, seen at an angle of  $42^\circ$  from the meridional direction.

In nylon 6 fiber, with a different hydrogen-bond mechanism, a similar signal is observed but in this case it is reported<sup>16</sup> as a combination of the 102 and 012 reflections. The calculated spacings of these two reflections are 0.62 and 0.56 nm, respectively which should be expected to be resolvable experimentally. Unfortunately no measured spacing is given in the original paper describing the structure of nylon 6.<sup>16</sup>

In our nylon 46 X-ray diffraction patterns from sedimented mats a strong reflection on the second layer line occurs at a measured spacing of 0.53 nm which corresponds to the calculated spacing (0.524 nm) of the 012 reflection in our proposed structure.

**4. The Fold in Nylon 46.** The stereochemistry of the fold itself will be reported in detail elsewhere.<sup>29</sup> Suffice to say that the planar amide group prefers to lie at an angle to the hydrogen-bonded sheet plane and there are four low-energy conformations to be considered. It has not escaped our notice that the amides in the folds have the potential to hydrogen bond successive sheets together and even influence the relative shear between sheets. This aspect of the structure and its implications for the crystallography, thermal behavior, and properties of nylon 46 is being currently investigated.

We know from the previous work on nylon 66<sup>10</sup> that nylon chains can fold in the alkane segments. It is sterically possible for nylon 46 to fold via the alkane segment. If it did so, a hydrogen-bond scheme similar to nylon 66 would occur in the straight-stem segments and the chains would lie at an angle to the lamellar normal. Thus *a priori* nylon 46 has a choice of folding patterns, and in crystals formed from the melt both possibilities might occur. Indeed, independent investigations on nylon 46 fibers indicate that both types of hydrogen-bond schemes for the straight-stem parts of the structure can exist in fibers.<sup>30,6</sup> The relationship between the folds in nylon 46, the internal organization of the hydrogen-bonded sheets, and the three-dimensional structure is currently under consideration jointly by ourselves and DSM.

**5. Folding in Nylons and Connection with Proteins.** For folds containing the amide group the equal number of CH<sub>2</sub> groups in the acid and amine portions in nylon 46 allows matching of the amide groups in the straight stems to form hydrogen-bonded sheets. Other nylons with equal numbers of CH<sub>2</sub> units in acid and amine portions, e.g.

nylon 68, also have the potential to form similar hydrogen-bonded sheets and bend with an amide in the fold.

Within the broader family of symmetrical nylons, as the number of CH<sub>2</sub> units between amide groups decreases, a change in the folding mechanism would be expected to occur. Clearly at some stage the alkane segments will be too short for folding anywhere else except in the amide group, which is the case for the proteins (chemically decorated nylon 2). Thus the folding behavior of nylon 46 makes a connection between two separate subject areas.

### Conclusions

Our experimental evidence shows that in nylon 46 crystals the chains lie normal to the lamellar surfaces and are hydrogen-bonded into sheets analogous to the proposed nylon 6 structure and antiparallel  $\beta$ -protein structure. There is no progressive shear of the chains within a sheet and between sheets as found in nylon 66 and its relatives nylon 6.10 and nylon 6.12. The crystalline core of the lamellar crystals index on a monoclinic unit cell with parameters  $a = 0.96$ ,  $b = 0.826$ , and  $c$  (the chain axis) = 1.47 nm and  $\gamma = 115^\circ$ , which contains two sheet segments (or four chain segments) and has a calculated density of 1.24 g/cm<sup>3</sup>. Consideration of the low-angle X-ray diffraction in relation to the wide-angle diffraction demands four chemical repeats and sharp (adjacent reentry) folds in the 6-nm-thick lamellae.

The observed crystal structure can only exist if the folds incorporate an amide group, rather than fold via the alkane segments. This folding geometry is wholly different from previous folding models reported for nylons. We believe that the discovery of this novel fold is the principal conclusion of the present work.

**Acknowledgment.** We wish to thank Dr. Wilbert Derks for providing us with useful information regarding nylon 46 fibers and to DSM for providing samples and financial support for part of the work.

### References and Notes

- (1) Coffman, D. D.; Berchet, G. J.; Peterson, W. R.; Spanagel, E. W. *J. Polym. Sci.* 1947, 2, 306.

- (2) Beaman, R. G.; Cramer, F. B. *J. Polym. Sci.* 1956, 21, 223.
- (3) Ke, B.; Sisko, A. W. *J. Polym. Sci.* 1961, 50, 87.
- (4) Gaymans, R. J.; Van Utteren, T. E. C.; Van Den Berg, J. W. A.; Schuyer, J. *J. Polym. Sci.* 1977, 15, 537.
- (5) *Fibres from synthetic polymers*; Hill, R., Ed.; Elsevier: Amsterdam, 1953.
- (6) DSM, Private communication.
- (7) Bunn, C. W.; Garner, E. V. *Proc. Roy. Soc., (London)* 1947, 189, 39.
- (8) Keller, A. *J. Polym. Sci.* 1959, 36, 361 (with an appendix by R. Engleman).
- (9) Dreyfuss, P.; Keller, A. *J. Makromol. Sci. (Phys. Ed.)* 1970, B4 (4), 811.
- (10) Atkins, E. D. T.; Keller, A.; Sadler, D. M. *J. Polym. Sci.* 1972, A2 (10), 863.
- (11) Dreyfuss, P.; Keller, A. *J. Polym. Sci.* 1970, B8, 253.
- (12) Burmester, A. F.; Dreyfuss, P.; Geil, P. H.; Keller, A. *J. Polym. Sci. (Polym. Letters)* 1972, 10, 769.
- (13) Hinrichsen, G. *Makromol. Chem.* 1973, 166, 291.
- (14) Dreyfuss, P. *J. Polym. Sci. (Polym. Phys. Ed.)* 1973, 11, 201.
- (15) Magill, J. H.; Girolamo, M.; Keller, A. *Polymer* 1981, 22, 43.
- (16) Holmes, D. R.; Bunn, C. W.; Smith, D. J. *J. Polym. Sci.* 1955, 17, 159.
- (17) Geddes, A. J.; Parker, K. D.; Atkins, E. D. T.; Beighton, E. J. *Mol. Biol.*, 1968, 32, 343.
- (18) Fraser, R. D. B.; MacRae, T. P. *Conformation in Proteins*; Academic Press: New York, 1973.
- (19) Schulz, G. E.; Schirmer, R. H. *Principles of Protein Structure*; Springer-Verlag: New York, 1987.
- (20) Blundell, D. J.; Keller, A.; Kovacs, A. *Polym. Lett.* 1966, B4 481.
- (21) Wittmann, J. C.; Lotz, B. *J. Polym. Sci., Phys.* 1985, 23, 200.
- (22) Organ, S. J.; Keller, A. *J. Polym. Sci.* 1987, B25, 2409.
- (23) Holland, V. F. *Makromol. Chem.* 1964, 71, 204.
- (24) Kovacs, A. J.; Lotz, B.; Keller, A. *J. Macro. Sci. Phys.* 1969, B3 (3), 385.
- (25) Astbury, W. T. *Trans. Faraday Soc.* 1940, 36, 871.
- (26) Pauling, L.; Corey, R. B. *Proc. Natl. Acad. Sci.* 1953, 39, 253.
- (27) Gaymans, R. J.; Doeksen, D. K.; Harkema, S. *Integration of Fundamental Polymer Science and Technology*; Kleintjens, L., Lemstra, P., Eds.; Elsevier: Amsterdam, 1986; p 573.
- (28) Derks, W. H.; Moonen, J. A. H. M.; Ramaekers, F. J. W.; Kooij, C. J. IUPAC Montreal, July, 1990; and the Physics Polymer Conference, Bristol, April, 1991.
- (29) Atkins, E. D. T.; Lee, I. Manuscript in preparation.
- (30) Keller, A.; Maradudin, A. *J. Phys. Chem. Solids* 1957, 2, 301.

**Registry No.** Stanyl (SRU), 50327-22-5; stanyl (copolymer), 50327-77-0.